2001ESASP.499..163C

Bidirectional Reflectance Factor Analysis from Field Radiometry and HyMap data

F. Camacho-de Coca, M. A. Gilabert and J. Meliá
Departamento de Termodinàmica. Facultat de Física. Universitat de València
Dr. Moliner, 50. 46100 Burjassot (Valencia) Spain
Phone: +34963983113 Fax: +34963983099 Email: Fernando.Camacho@uv.es

INTRODUCTION

Vegetation canopies like most of the natural surfaces reflect the incoming radiation flux in an anisotropic way. Thereby, for an adequate interpretation of the reflectance, we should geometrically characterise the reflecting properties of the surfaces. The basic function that characterises the angular dependence of the reflectance is the Bidirectional Reflectance Distribution Function (BRDF), which is -by definition- a non-measurable quantity due to involving infinitesimal solid angle, and therefore without measurable radiation, for all existing geometries [1]. However, we can estimate the BRDF of natural surfaces by means of the Bidirectional Reflectance Factor (BRF), which is defined for conical solid angle, and so involves measurable radiation quantities, for a limited set of all possible geometries.

From the last decade up to now, the interest in the characterisation of the BRDF from space has been on the increase in Space Agencies. Sensors such as the POLarization and Directonality of the Earth´s Reflectance (POLDER) or the Multi-Angle Imaging Spectro Radiometer (MISR) have been developed able to observe the Earth from off-nadir angles. In particular, the POLDER optical concept is the most suitable for the estimation of the BRDF from space [2], although for a limited number of solar zenith angles range. On the other hand, the synergistic use of sensors on board geostationary satellites, like the forthcoming Spinning Enhanced Visible & InfraRed Imager (SEVIRI) on Meteosat Second Generation (MSG), and on board polar orbiting platform like the Advanced Very High Resolution Radiometer (AVHRR-3) on European Polar System (EPS) will allow an increase angular sampling of the targets and a better characterisation of the BRDF. SEVIRI will provide daily sampling for different sun zenith angle although always with the same view zenith angle, while AVHRR-3 will provide viewing variations close to the principal plane using a set of several days [3].

The major interest in estimating the BRDF for vegetation canopies studies is found in the fact that the anisotropic behaviour is related to the canopy geometry, among other factors. Consequently, the anisotropic behaviour that it shows in the BRF, when the viewing geometry changes, depends on the canopy structural parameters. Nevertheless, the optical properties and the sun zenith angle must be taken into account for an adequate explanation of the bidirectional phenomenon [4], [5]. The dynamics of the BRF are controlled by the shadow's pattern and the proportion of sunlit components that are 'seen' by the sensor's field of view. These sunlit and shadows areas are connected with the aforementioned canopy geometry, optical properties and sun zenith angle by means of two effects: the *gap effect* and the *backshadow effect* [4], [6].

Vegetation components at the top of the canopy receive grater irradiance and hence scatter a larger amount of solar flux towards the sensor than the components at the bottom of the canopy. The gap effect is produced when increasing off-nadir view angle and the proportion of well-illuminated upper canopy component viewed from the sensor's field of view increases. Obviously, this effect is clearly related to the vertical structure of the canopy and the spatial distribution of elements which determines the fraction of soil, vegetation and shadows in the scene –for an specific sun zenith angle-. Backshadow effect is related to the orientation of the canopy components and the irradiation condition derived from the cosine law and shadow's pattern. Thus, when the normal of the surface is pointing to the sun the surfaces are more irradiated. This effect is very strong in the soils due to the fact that the single scattering governs the dispersion of radiation. Furthermore, the very low transmittance produces very dark shadows, increasing the contrast between the illuminated and shadowed facets. On the other hand, the optical properties of the vegetation determine the wavelength dependence of the anisotropy reflectance. For example, through its influence on the backshadow effect when single scattering govern the dispersion of radiation the effect is similar to that in soils. However, when the multiple scattering processes appear a diffuse radiation, which has the opposite effect, reducing the influence of the backshadow effect on the canopy. Finally, sun zenith angle determines the distribution of the irradiance. The sun near nadir favours isotropic scattering and reduces the shadows, while a near horizon position has the opposite effect and favours the anisotropic behaviour of the BRF.

On the principal plane, the combination of both, gap and backshadow, effects produce a broad reflectance increase or gradient of the reflectance constituting a directional signature with useful information about canopy structure [7] and LAI [8]. However, the hot spot effect, which occurs when the observation and the illumination directions are colinears, produce a much sharper increase over a very narrow region. This increase constitutes the hot spot signature, characterised by its amplitude and width, and is generally interpreted as a coherent transmission into the canopy [9], providing information of the ratio between horizontal (leaf scale) and vertical scales (canopy scale) of the canopy.

© European Space Agency • Provided by the NASA Astrophysics Data System

2001ESASP.499..163C

Theoretical models have shown that the hot spot width depends on the size of the leaves [10], the LAI [11] or a simple relation between the LAI, size and height of the cover [9]. The amplitude of the hot spot peak of a dense canopy has been related to the reflectance of a single leaf [9]. However, it is very difficult to obtain the shape of the hot spot peak since a very high angular resolution is necessary that in some cases can be lower than 0.5°. The Hot Spot Signature has been under-exploited as yet due to the specific geometry conditions and the angular requirements. Nevertheless, works from POLDER reveals less information than we could expect from the theoretical model [9].

On the other hand, the wide FOV sensors utilised for monitoring vegetation like the AVHRR or the VEGETATION are much influenced by the viewing geometry. This implies that vegetation products like vegetation indexes or biophysical parameters such as the LAI or the fAPAR, which play a fundamental role in models for the estimation of land-atmosphere processes, will be affected by anisotropic behaviour, and so the anisotropic effects should be suitably corrected

In this framework, the DAISEX 1999 campaign provides us with an exceptional opportunity to study some of the main aspects of the aforementioned BRDF effects from field measurements and the wide-FOV HyMAP airborne data. In particular, flights carried out with the DLR Do228 airborne allow us to study the variability in the reflectance of different natural surfaces in the two extreme viewing planes, the principal plane and the orthogonal plane, and for three different sun zenith angles. Furthermore, the hyperspectral capabilities of both GER-3700 and HyMAP provide useful information to discuss the wavelength dependence of the anisotropic behaviour, an aspect which must give us useful information to be taken into account for future multi-angular sensors spectral capabilities.

This bidirectional reflectance factor analyses has been made in order to:

- determine the viewing geometry influence for choosing the most suitable configuration for validation purposes, this being the main task of the field radiometry group of the University of Valencia. For this purpose, field and HyMAP airborne measurements from orthogonal and principal plane have been used.
- show differences in the angular signature of dense vegetation canopies due to their structural parameters. For this purpose a previous study for the adequate selection of the samples has been made from field radiometry.
- evaluate the capability of HyMAP instrument to acquire the hot spot directional signature, and to check the possibility of retrieving structural information from this.
- quantify the sun zenith angle influence over spectral response of natural surfaces and to study the utility of the forthcoming high temporal frequency data under fixed observation angles from two perspectives, similarity with viewing angles variation (reciprocity principle) and complementary information due, for example, to moisture changes.
- analyse the wavelength dependence of the anisotropy reflectance introduced by changing view and sun zenith angle, and its implications for future multi-angular and multi-spectral missions.

METHODOLOGY

Anisotropic behaviour of the reflectance is mainly governed by the sun-target-sensor geometry that determines the shadow's pattern view by the sensor. Figure 1 shows the geometry of the incident and reflected radiation beams.

φ_i defines the position of the principal plane, which contains the source. φ_r defines the view plane position and the azimuth relative angle $\Phi=\varphi_i-\varphi_r$ indicates the view plane position with respect to the principal plane. We can determine the viewing geometry by the view zenith angle and the view plane. Thereby, the sun-target-sensor geometry is characterised by the viewing geometry and the sun zenith angle. For each azimuth plane we have two contributions to reflectance, one with positive view zenith angle (back to the sun) and the other one with negative view zenith angle (facing the sun), corresponding to both view azimuth angles that determine the same view plane.

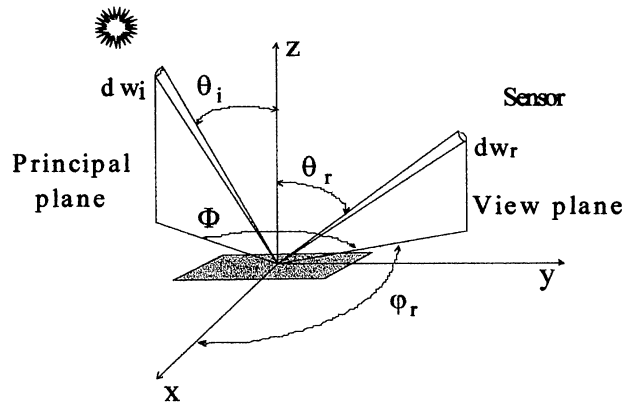

Fig1.Coordinate system defining geometry of incident and reflected elementary beams: dω (solid angle element), θ (zenith angle), φ (azimuth angle), i (illumination direction), r (viewing direction) and Φ (azimuth relative angle).

In order to quantify viewing geometry influence on reflectance of different targets a unique spectral anisotropy quantity is required. The anisotropy index (ANIX) gives the amplitude of the reflectance variation for a defined azimuth angle and sun zenith angle [6]:

$$ANIX(\lambda)=\frac{R_{MAX}(\lambda)}{R_{MIN}(\lambda)} \quad (1)$$

where R_{max} is the maximum reflectance factor and R_{min} the minimum

© European Space Agency • Provided by the NASA Astrophysics Data System

2001ESASP.499..163C

In order to analyse the wavelength dependence of the anisotropy reflectance, we use the simple anisotropy factor (ANIF) which is a normalisation with the nadir reflectance [6]:

$$ANIF(\lambda,\theta_i,\varphi_i,\theta_r,\varphi_r)=\frac{R(\lambda,\theta_i,\varphi_i,\theta_r,\varphi_r)}{R_0(\lambda,\theta_i,\varphi_i)} \quad (2)$$

where R_0 is the reflectance factor acquired from nadir view.

For the analyses of the anisotropy effects of the reflectance due to illumination conditions it is also convenient to have an anisotropy factor that makes reference to illumination angle variation. For this reason, we have introduced an anisotropy factor related to the illumination condition (ANIF*i*) as follows:

$$ANF_i(\lambda;\theta_i,\varphi_i,\theta'_i,\varphi'_i;r)=\frac{R_r(\lambda,\theta_i,\varphi_i)}{R_r(\lambda,\theta'_i,\varphi'_i)} \quad (3)$$

where *r* represents the viewing direction. For practical purposes we thought that the nadir view is the most adequate and where it is assumed revolution's isotropy in the reflectance, thereby the expression (3) becomes to simplest form (4):

$$ANIF_i(\lambda,\theta_i,\theta'_i)=\frac{R_0(\lambda,\theta_i)}{R_0(\lambda,\theta'_i)} \quad (4)$$

where R_0 is the reflectance acquired from nadir.

Samples description

In order to achieve the aforementioned objects of this work a selection of the most adequate samples has been made. Some of these like V1 and V17 are selected for their structural difference. Some like S10 and S2 are selected for validation purposes, others like V14 and V16 are chosen from HyMap as they show the hot spot effect. Finally V11 and SV3 are also included in the illumination analysis from HyMAP to increase variability in the LAI. The main characteristic of these surfaces is shown in table 1.

The main difference between soils is their roughness: S10 is a smooth surface with low roughness, in contrast S2 exhibit very large furrows and high roughness. V1 corresponds to a very dense and ripe wheat crop with spikes about 90 cm in height. The erectophile distribution of the spikes differs drastically from alfalfa, V17, cover corresponds to a planophile and very dense (LAI around 3.0) alfalfa cover of height between 50 and 60 cm.

On the other hand, from airborne data we have also studied the bare soil S10, the V1 and V17 dense canopies. Furthermore, we have included the irrigated barley, V11, and the spare vegetation cover of sugar beet, SV6 with similar LAI but different structure (barley has an erectophile distribution and sugar beet has very broad leaves and planophile distribution) and phenology. The analyses of the hot spot signature has been made with the alfalfa, V16, field that corresponds to a complete canopy of similar characteristics to V17. The adjacent alfalfa, V14, which has similar characteristic to V16, is also studied for increasing the view zenith angle range from HyMAP imagery.

The study area is encompassed in a 790 x 790-pixel window made from upper left coordinate UTM: 576347.5E, 4325432.5N.

Table 1. Main characteristic of the samples studied in this work

Name	Description	LAI	Height (m)
V17	Alfalfa	3.6	0.5-0.6
V1	Wheat	1.8	0.9-1.0
V14	Alfalfa	3.4	-
V16	Alfalfa	4.2	0.6-0.7
SV6	Sugar beet	0.8	0.1-0.15
V11	Barley	0.6	-
S10	Smooth soil	-	-
S2	Rough soil	-	-

Field Radiometry data

For this study different measurements of field radiometry data have been used. On one hand, the University of Valencia (UV) took measurements for validation purposes, simultaneously to the flights and throughout the day, over S2 and S10 bare soils that can be used to analyse diurnal variability in the reflectance. Furthermore, angular sampling was performed in a limited set of viewing geometries over alfalfa, V17, and wheat, V11, vegetation canopies and the S2 soil to study the difference in the angular signature. The UV measurements used in this study appear in tables 2 and 3. Solar angles have been obtained according to Iqball equations [12]. The methodology of acquisition of angular measurements is illustrated in plate 1.

In addition, we have completed the analyses of field data with some of the goniometer sampling acquired with the FIGOS (Field Goniometer System) by the University of Zurich (UZ). The measurements utilised correspond to angular measurements of the bare soil, S10, in both the principal and orthogonal planes (see table 4).

Table 2. Field Radiometry measurements from nadir view of the University of Valencia used in this study. Date=990604 SLT (Solar Local Time), SZA (Solar Zenith Angle) and SAA (Solar Azimuth Angle).

S10 (Bare soil)			S2 (Bare soil)		
SLT	SZA	SAA	SLT	SZA	SAA
7:22	61.8°	82.9°	7:07	65.1°	80.4°
8:13	52.3°	90.6°	7:56	55.7°	87.9°
12:41	18.1°	204.8°	12:24	16.9°	193.9°
14:30	34.2°	251.7°	14:14	31.5°	248.1°
15:15	42.8°	259.8°	15:05	40.9°	261.6°

© European Space Agency • Provided by the NASA Astrophysics Data System

2001ESASP.499..163C

Table 3. Angular measurements of the University of Valencia that it has been used in this study.

	S2 (Bare soil) (99/06/04)			
	Principal Plane		Orthogonal Plane	
	Start	End	Start	End
SLT	10:51	11:25	-	-
SZA	23.6°	18.9°	-	-
SAA	129.4°	148.2°	-	-
	V1 (Wheat) (99/06/05)			
	Principal Plane		Orthogonal Plane	
	Start	End	Start	End
SLT	9:10	9:30	9:35	10:15
SZA	41.5°	37.5°	36.8°	29.1°
SAA	101.1°	104.5°	106.0°	115.9°
	V17 (Alfalfa) (99/06/05)			
	Principal Plane		Orthogonal Plane	
	Start	End	Start	End
SLT	10:45	11:01	11:10	11:32
SZA	24.3°	22.1°	20.8°	18.3°
SAA	127.1°	134.4°	138.6°	152.2°

Table 4. Angular measurements made with FIGOS by the University of Zurich that it has been used in this study. Date: 99/06/03.

	S10 (Bare Soil)			
	Principal Plane		Orthogonal Plane	
	Start	End	Start	End
SLT	08:38	08:46	08:54	08:58
SZA	47.3°	45.8°	43.3°	42.7°
SAA	94.9°	96.7°	97.7°	98.5°

HyMAP airborne data

In order to study the anisotropic reflectance behaviour over natural vegetation canopies from airborne data, we have used the HyMap data acquired in Daisex-99 campaign on 3 and 4 June 1999. During this campaign, 6 flights over the Barrax area were carried out with the wide FOV HyMap instrument on board DLR Do228. Flights were designed to show illumination and viewing influence over radiometric response and to record the hot spot phenomenon in Hymap imagery. Two perpendicular flights were carried out in the morning, at noon and in the afternoon, (see table 5). Flight configuration allows us to analyse illumination conditions influence over reflectance and derived products.

HyMap provides 128 channels between 0.4 y 2.5 μm, with 5m spatial resolution and 60 degrees swath width, so we can also study view angle effects influence under several viewing geometries along optical spectrum. HyMap is a cross-track scanner. Therefore, in order to acquire the hot spot phenomenon the flight direction should be perpendicular to the principal plane. Furthermore, the solar zenith angle must be less than 30 degrees and, of course, the radiometric sensibility should be suitable and not saturate near the hot spot value.

In table 5, the image called Bar2_12 is the unique configuration that allows us to obtain the hot spot effect, due to scan direction is in the principal plane and the sun zenith angle is lower that ½FOV. A scheme of the Bar2_12 geometry is shown in figure 2. For all flights, solar azimuth angle (SAA) is close to a cardinal point, East in the morning flight, South in the noon flight and West in the afternoon flight. Flight tracks were orthogonal among them following South to North or East to West direction, and then for each solar position we have two images: one acquired near the principal plane and the other acquired near the orthogonal plane, as observed below. The images were atmospherically and geometrically corrected at DLR.

Table 5. Flights over the Barrax test site. SLT (Solar Local Time), SZA (Solar Zenith Angle), SAA (Solar Azimuth Angle). Bar1 do reference to south-north wards flights and Bar2 to east-west wards flights.

NAME	Date	SLT	SZA	SAA
Bar1_12	990603	11:52	17.8°	168.9°
Bar2_12	990603	12:08	17.6°	182.1°
Bar1_08	990604	08:01	54.4°	89.5°
Bar2_08	990604	08:16	51.5°	92.0°
Bar1_15	990604	14:58	40.0°	257.4°
Bar2_15	990604	15:11	42.5°	260.5°

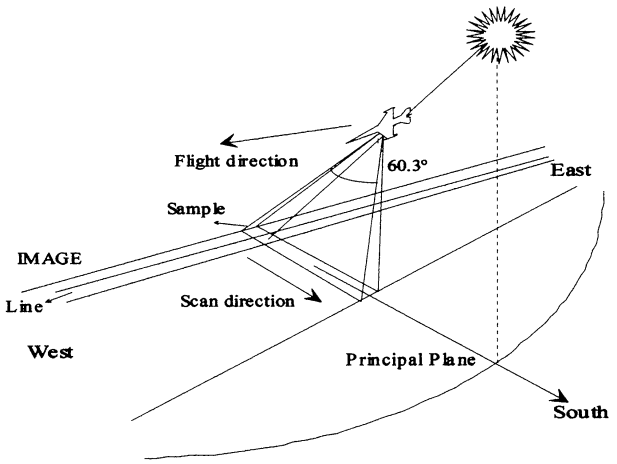

Fig. 2 Scheme representative of image acquisition in the hot spot configuration.

In order to check the HyMAP capabilities to retrieval information of the hot spot signature we have calculated the angular width of the hot spot peak (γ), [9], defined as follows:

$$\gamma \cong LD/7H \qquad (5)$$

© European Space Agency • Provided by the NASA Astrophysics Data System

2001ESASP.499..163C

where L is the LAI, D is the diameter of the leave, and H is the height of the cover.

RESULTS

Field data

a) Viewing geometry

Firstly, we have analysed the UV angular measurements made on the complete wheat (V1) and alfalfa (V17) cover in order to find differences in the angular signature due to the canopy structure. Plate 2 shows the nadir view of both fields where canopy geometry is illustrated for a better understanding of the bidirectional effects.

Figure 3 shows the variation of the BRF along the orthogonal plane regarding view zenith angle. Both graphs show high degree of symmetry with respect to the nadir view, as a consequence of the symmetric shadow's pattern that is seen by the sensor at this specific viewing plane. Nevertheless, both covers exhibit differences between them. On one hand, the alfalfa cover shows slight reflectance variations when the view zenith angle changes, which can be attributed to spatial heterogeneity, as we can observe in plate 2 and, in general, there is little influence of the view zenith angle. On the other hand, the wheat cover exhibits an increasing trend of the reflectance when the view zenith angle increases.

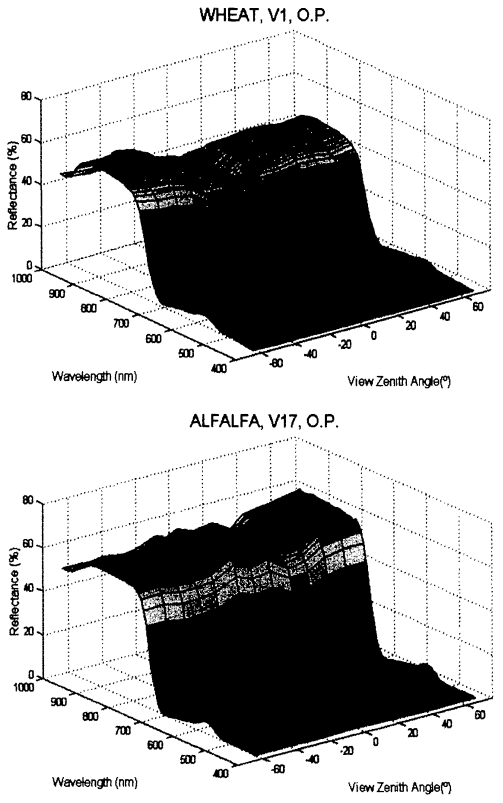

Fig. 3. Bidirectional Reflectance Factor *vs.* View Zenith Angle in the Orthogonal Plane: a) Wheat (V1), SZA=34°, b) Alfalfa (V17), SZA= 19°

The lowest value of the BRF is at the nadir view, where the lower layers less illuminated can be seen, while the maximum values are at the most extreme view zenith angle, where the upper and more illuminated layers of the canopy are seen. Consequently, the gap effect is more important in this cover, which is less dense and higher than the alfalfa cover. The anisotropy index for the wheat V1 cover at 550 nm is of about 1.4, *id est,* the reflectance factor at 64° in the orthogonal plane increase the nadir value at 550 nm (for an specific SZA of 33°) by 40%.

There are several factors that contribute to the fact that the gap effect has a major influence on the wheat than on alfalfa. On one hand, the wheat shows an erectophile structure due to it being completely spiked, while alfalfa has a planophile distribution with broad leaves favouring isotropic scattering. On the other hand the SZA is different, for the wheat canopy this was around 33° while for the alfalfa it was around 20°. Thereby, for the wheat measurements the sun zenith angle favoured a gradient of interception of radiation between upper and lower layers, in contrast with the alfalfa canopy where the sun zenith angle was lower allowing a more homogeneous irradiation of the cover.

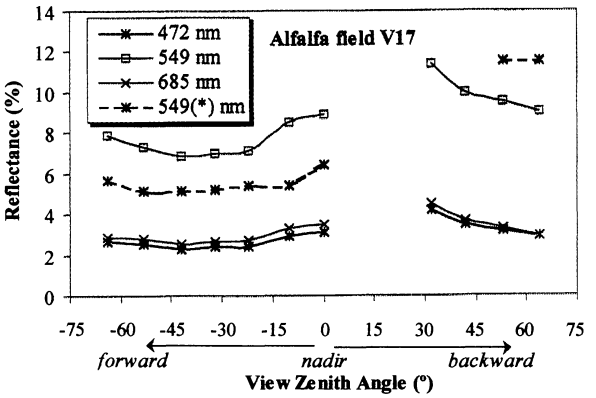

Fig. 4. BRF *vs.* view zenith angle in the principal plane for the alfalfa V17 canopy, SZA=23° and for the wheat V1 canopy only at 549(*) nm, SZA=40°

Figure 4 shows partially the angular signature in the principal plane, which is related to the canopy geometry. We can refer to this angular signature as the '*broad hot spot signature*' due to it is acquired in the principal plane (hot spot azimuth angle condition) but far from the backscattering region (hot spot zenith angle condition). Despite that the hot spot region, which contains the highest values of the BRF, could not be measured because of experimental constrains, the anisotropic behaviour of the BRF in this plane is clearly manifested. In order to understand the missing information in the hot spot region we are going to use the HyMap data.

For the alfalfa cover, the angular signature in the forward scattering reaches the minimum at medium angles increasing for the extreme view angles. This trend, that does not occur for soils, was already reported in the dense covers from laboratory, [5], [6], and field radiometry data, [4], and it is a consequence

© European Space Agency • Provided by the NASA Astrophysics Data System

2001ESASP.499..163C

of the gap effect. For the wheat cover the behaviour is different as a consequence of its canopy geometry. A very linear behaviour can be observed and the reflectance increases only for the most extreme angle. This result seems to be in disagreement with the gap effect, which has been shown to be more important for the wheat canopy in the orthogonal plane. However, the directional signature is a combination of the gap and the backshadow effect, which is much more important in the wheat cover. Vertical structure, the higher sun zenith angle and the optical properties of the spike, which shows strong opacity, produce very dark shadows in the forward scattering, which furthermore receive less irradiation due to cosine law and the erectophile distribution of the spike. Consequently, the differences between the upper and the lower layers in the forward scattering are negligible, reducing the gap effect. However, it has been proved that in the NIR region, where multiple scattering reduce the backshadow effect, the wheat reflectance in the forward scattering shows major gap effect than alfalfa in agreement with the orthogonal plane results.

For the bare soil study, we firstly present the chosen angular measurement for the bare soil, S10, obtained with the FIGOS.

Figure 5-a) shows a very asymmetrical behaviour of the reflectance in the principal plane regarding the reflectance at nadir.

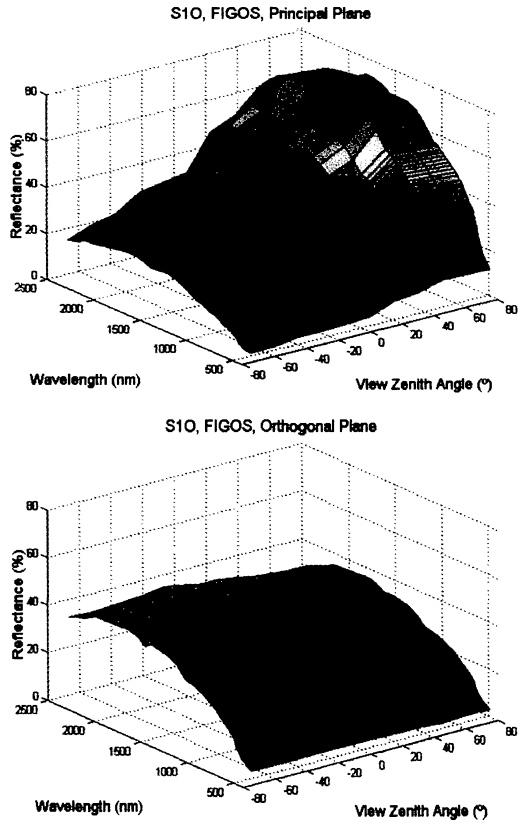

Fig.5 Bidirectional Reflectance Factor (from UZ) *vs.* View Zenith Angle for the smooth red clay soil, S10. Sun Zenith Angle ≅ 45°

At the backscattering region, the BRF increases as the view zenith angle increases to 45° while in the forward scattering the effect is opposite and the BRF decrease when the view zenith angle increase, showing the lowest values at 75° forward.

However, the hot spot cannot be measurement from field data due to the shadow of the sensors (this is particularly manifested in the University of Valencia measurements). Another issue is the angular resolution necessary to obtain the shape of the hot spot peak, which must be as fine as possible. Thereby, the measurements acquired with the FIGOS (15° zenith angular resolution in this campaign) prevent us from knowing the shape of the hot spot with the necessary precision. In contrast, these measurements allow us to study the gradient in the BRF and the broad hot spot signature and quantify the anisotropy existing in the reflectance at this angular resolution. The ANIX at 550 nm reaches a value of 3.6, which is a considerably high anisotropic behaviour for a smooth soil with low roughness.

On the other hand, figure 5-b) shows isotropic behaviour of the BRF in the Orthogonal Plane although with slight variations. This behaviour is quantified again with the anisotropy index that is at 550 nm of 1.2, very close to the isotropic behaviour. This deviation could be produced by a small deviation of the orthogonal plane, and not to sun position variation due to the fact that measurements were acquired very quickly. The isotropic behaviour in smooth soil in the orthogonal plane is an expected result having in mind that the soils have not a pronounced vertical scale. Consequently, the gap effect is not manifested in soils, and when the view angle increase in the orthogonal plane the proportion of shadows and sunlit components remains practically constant.

This isotropic behaviour in the orthogonal plane is produced despite the low sun position, which favours the anisotropic behaviour due to increasing shadows, so it is the ideal viewing plane to reduce view zenith angle influence. Consequently, we have chosen this view plane in order to carry out the validation of the wide-FOV, DAIS and HyMap, airborne data.

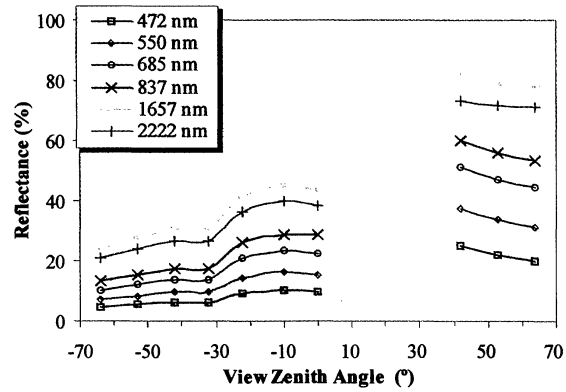

Fig. 6. Bidirectional Reflectance Factor at different view zenith angle in the principal plane. SZA=24°

© European Space Agency • Provided by the NASA Astrophysics Data System

2001ESASP.499..163C

Figure 6 shows the broad hot spot signature in the rough soil, S2. The gap in the angular sampling due to the shadow of the UV sensor platform can be observed. This figure very clearly shows several aspects. Firstly, strong difference between forward and backward reflectance, which produced an anisotropy index value at 550 nm of 5.5, higher that the 3.6 for S10 with similar sun zenith angle, due to the higher roughness of S2. Secondly, there is no influence of the gap effect despite the high roughness of the surface. The anisotropic behaviour in soils can be mainly interpreted by the backshadow effect. Finally, for all the wavelengths the angular signature presents no difference. This is related to the optical properties of the soil, an aspect discussed in section c.

b) Sun Zenith Angle

From field radiometry data, the sun zenith angle influence has only been studied for the soils, S2 and S10, which were selected for validation purposes, and also to shows the effect of roughness on the BRF. To do so, the measurements were acquired at nadir view throughout the day, i.e., with different sun zenith angles. Figure 7 shows the diurnal variability existing in the spectral signature of the S2 field.

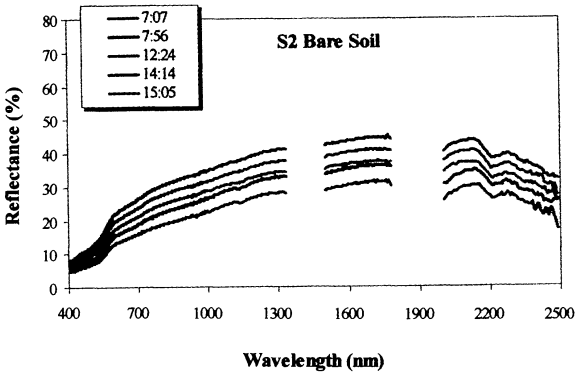

Fig. 7. Spectral Signature for S2 field at different solar local time.

The lowest reflectance value corresponds to the highest SZA (in the morning), while the maximum value is for the lowest SZA (at noon). In this case the increasing SZA produces a higher proportion of shadowed elements and, in consequence, a diminishing value of the reflectance. Similar results occur with the smooth soil, S10, although with less intensity because of its lower roughness. The anisotropy index at 550 nm is 1.7 for the rough soil, S2, and 1.4 for S10. Wavelength dependence is studied below.

c) Wavelength dependence

Another point of interest in this discussion is to evaluate the wavelength dependence of the anisotropy reflectance, bearing in mind the determination of the optimal number of channels in a multi-angular sensor for land studies. In order to perform this analyse we have made use of the anisotropy factor (ANIF).

The following figure shows the highest ANIF for the field (soils and vegetation) studied. This anisotropy, which is consequence of the viewing geometry, has been obtained in the principal plane.

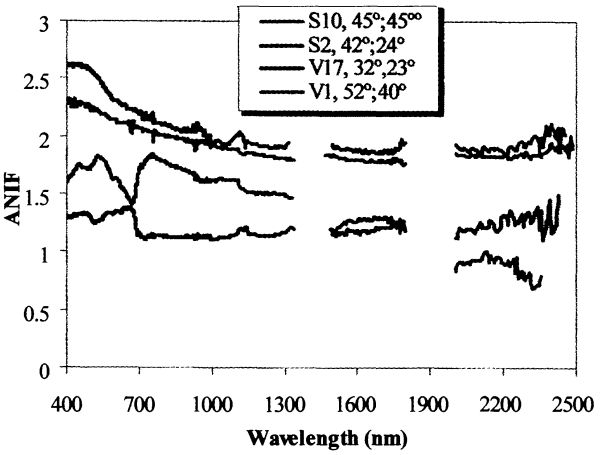

Fig. 8. Wavelength dependence of Anisotropy factor. The legend informs us about the sample name, the view zenith angle and the SZA.

For the soil fields, S2 and S10, the ANIF wavelength dependence is similar. The highest values correspond to the rougher S2 soil. The trend with the wavelength is related to the absorbance of the soil. Thus, only where the absorbance is higher, and there is more contrast between shadows and sunlit facets, the ANIF increases more quickly, mainly in S2 due to there is a major proportion of shadows. This behaviour indicates that a few bands can be enough to characterise the anisotropy reflectance of soils.

For the alfalfa V17 canopy, the ANIF shows a similar spectral behaviour as other complete vegetation cover studied from laboratory data, [5], [6]. This wavelength dependence is characterised by the multiple scattering influence, thereby in the red and blue bands the anisotropy shows a peak mainly in the red one, while in the NIR region the anisotropy is reduced. Therefore, the wavelength dependence of the ANIF is directly related to the variation of the optical properties along the spectral range. This suggests that for the spectral characterisation of the anisotropy reflectance of vegetation canopies, the multi-angular sensors should have at least one band for each spectral region where vegetation optical properties have different behaviour.

For the wheat canopy, the anisotropy wavelength dependence is completely different showing an inverse trend. For the alfalfa canopy, the ANIF is lower where multiple scattering govern the dispersion processes in the canopy. However, in these regions the ANIF for the wheat canopy shows the highest values. On the other hand, in the near infrared region the anisotropy factor is not wavelength independent as in the alfalfa and previous studies, and shows a decreasing trend, which is more evident where the water absorption is more important. In order to interpret this difference, we have to take into account the canopy geometry, the SZA and the phenology of the crop. In this case, the wheat has complete cover but the LAI is half that of the alfalfa. The spike in the wheat is formed and the leaves

© European Space Agency • Provided by the NASA Astrophysics Data System

2001ESASP.499..163C

have lost vigour. Therefore, the ANIF for wheat shows mainly the characteristic of the spike. For that, the water content of around 60% in the spike[1] it is noted in the ANIF as a consequence of the higher proportion of spikes in upper layers, and the gap effect. In the alfalfa canopy, where leave water content is around 80%, this effect is not appreciated due to planophile distribution, and the low SZA. Consequently, and although SZA are different for alfalfa and wheat canopy, the difference in the anisotropy wavelength dependence has shown the high structural parameters difference between the two. The ANIF has shown a water absorption influence in a cereal canopy, and further research should be performed in order to determine the usefulness of this information and the convenience of adding these bands to the future multi-angular missions.

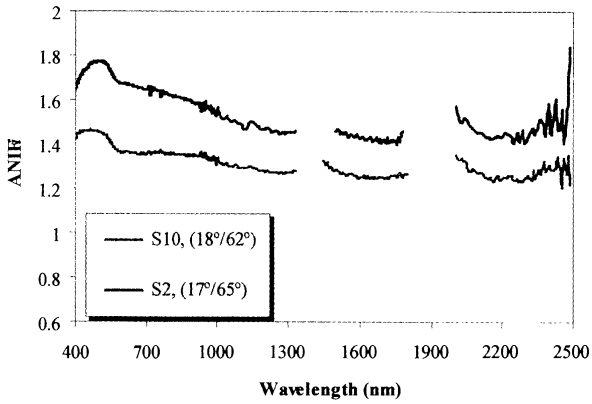

Fig 9. Anisotropy factor due to the illumination angle. Legend indicates field, and SZA involves in the calculation.

The ANIF*i* from field data is shown in figure 9. The wavelength dependence shows the same behaviour as in the ANIF. However to normalise the nadir reflectance for the ANIF*i* we have used R_0, in the morning corresponding to the highest SZA, *id est*, the opposite of the ANIF calculation. This result shows good agreement with the reciprocity principle.

HyMap data

The HyMap data has been used mainly to analyse the Hot Spot Signature, which could not be measured from field data, and to study the SZA influence over several vegetation canopies (and bare soil). The different images have been used to quantify the influence of the sun-target-view geometries on reflectance factor.

a) Viewing geometry

The maximum divergence for vegetation canopies between the orthogonal plane and the principal plane takes place when the hot spot effect appears. For this reason and prior to analysing the hot spot shape we have compared both images acquired at noon.

Figures 10 show a colour composition of Hymap images, Bar2_12 and Bar1_12, over the study area at noon flights. Figure 10-a corresponds to south-north wards flight scanning in a view plane very close to orthogonal plane, sun azimuth angle was about 169°. Figure 10-b corresponds to east-west wards flight scanning in the principal plane due to sun azimuth position being in the South and HyMap scan is across-track.

These images offer strong differences demonstrating viewing geometry influence over reflectance factor, so it is clear that

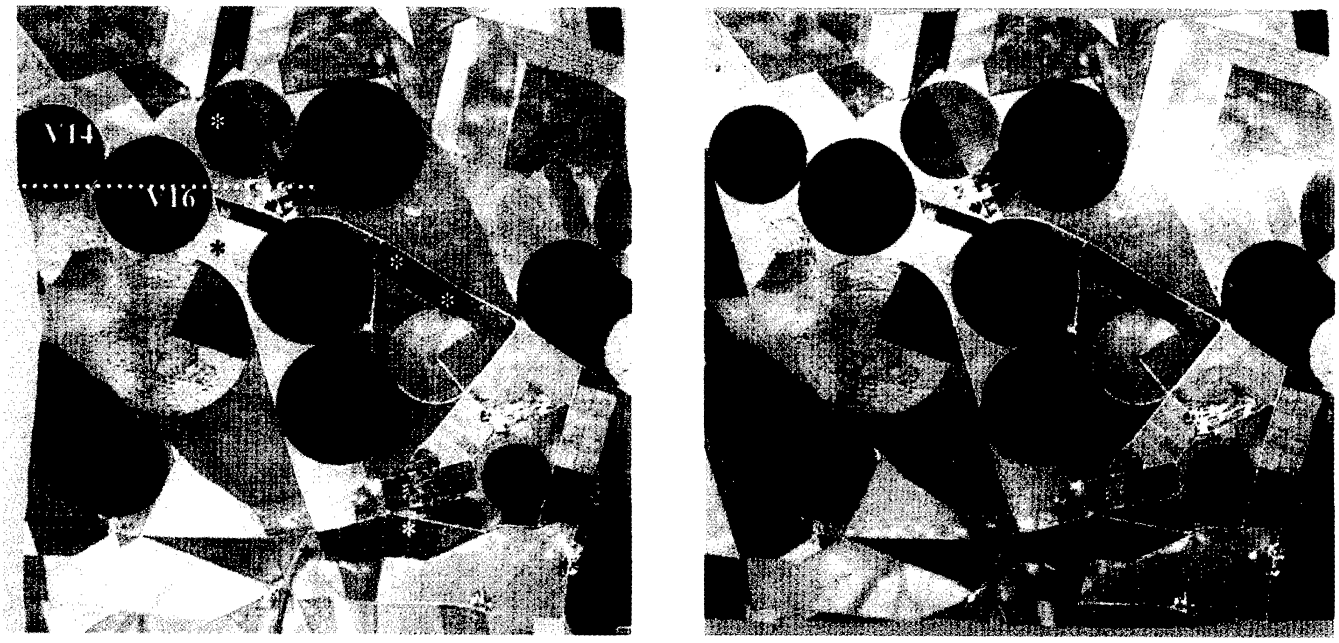

Fig.10 Images acquired over the study area at noon: a) Bar1_12, b) Bar2_12, where we can appreciate the hot spot effect. Dotted lines indicate the location of the profiles plotted in figure 11. Asterisk indicates the location of the studied samples.

© European Space Agency • Provided by the NASA Astrophysics Data System

2001ESASP.499..163C

these differences will produce divergences when used to obtain magnitudes derived from the reflectance, such as spectral vegetation indices. A visual inspection reveals that major differences between them are at the top of the image.

In the Bar2_12 image, acquired in principal plane, a bright band appears which is the hot spot effect over an HyMap airborne imagery. Bar2_12 corresponds to the geometry represented in figure 2; reflectance from the forward scattering, which has higher proportion of shadowed areas, is pictured at the bottom while reflectance from the backscattering, which has a lower proportion of shadowed areas, is pictured at the top. It is at the retro-solar direction where the illuminated faces of the surface conceal shaded faces, since radiance reflected in this direction is highest.

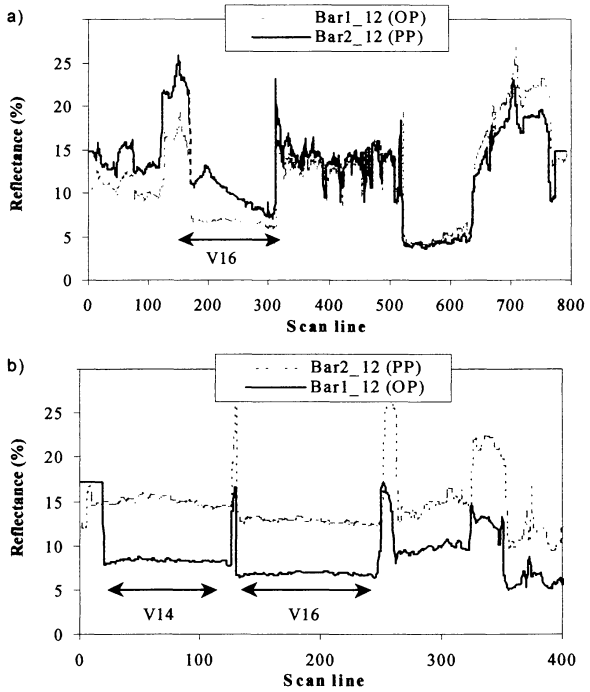

Fig. 11 a) Reflectance vs. View Zenith Angle (VZA) in the principal plane (PP). In dotted grey line the equivalent response for the orthogonal plane (OP) at VZA=14°, b) Reflectance vs. VZA in the OP. In dotted grey line the equivalent response for the PP at VZA=16°. Both of them are for the band 9 (549 nm)

Figure 11 compares the reflectance values at 549 nm of a selected sample in the principal plane (Bar2_12), which crosses the pivot-irrigated system of alfalfa field V16, with the corresponding values for the orthogonal plane (Bar1_12 image). For the Bar2_12, the view zenith angle is changing from 30° degrees backward at the top of image to 30° forward at the bottom. Scan lines begin at the top of image then the scan line goes from back to forward scattering (from +30° to –30° in the adopted criterium). In the orthogonal plane, due to the fact that the flight direction is perpendicular to the principal plane, the view zenith angle is constant. In general, figure 11-a) shows that in the principal plane off-nadir view over-estimates reflectance with respect to nadir-view in the backscattering and sub-estimates in the forward scattering independently of the type of surface, which is in agreement with previous works and the physical mechanisms aforementioned.

Figure 11-b) shows the view zenith angle variation in the orthogonal plane, only from 30°-view to nadir view, and it is compared with the corresponding values in the principal plane, where the VZA is constant. We can see that the two homogeneous alfalfa canopies such as the reflectance in the orthogonal plane and in the principal plane shows the same trend, although in the PP the reflectance values are higher due to viewing zenith angle. This result is also in agreement with the isotropic behaviour of the BRF in the orthogonal plane for very dense vegetation canopies. Consequently, this is the ideal configuration to minimising the viewing angles effects on the reflectance.

b) The Hot Spot effect

As we can see in the figure 11-a), for the PP the reflectance in the V16 region shows a very rapid increase in a very narrow region, which is the hot spot effect. For this analyses we have not taken into account the atmospheric effects over the hot spot signature. This effect must be carefully analysed although we thought that the hot spot signature has been hardly affected by the aerosol scattering of the solar radiation due to the good agreement between the anisotropy factor obtained from field and airborne data.

Figure 12 shows the hot spot effect over the alfalfa field V16. The equivalence with the view zenith angle has been calculated for one sample formed of 770 lines, corresponding to the HyMap FOV. Therefore, we have estimated an equivalence of 0.0783° by line, different from the IFOV of HyMap due to the geometrical correction of the image, so we can ascertain the view zenith angle for each pixel directly from the acquisition line. In this case, the V16 alfalfa field is located between the lines 169 and 308, thus the alfalfa pivot encompasses 10.8° of the angular HyMap FOV, with a very high angular resolution.

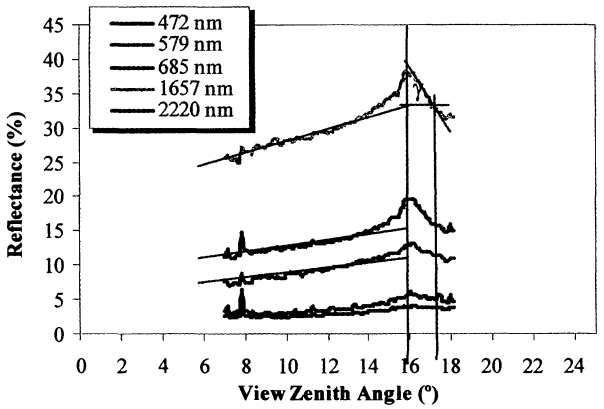

Fig. 12. Hot Spot signature at different wavelength for the alfalfa (V16) field. γ represents the width of the hot spot.

© European Space Agency • Provided by the NASA Astrophysics Data System

2001ESASP.499..163C

Maximum reflectance (hot spot peak) is observed in line 196, i.e. 199 lines from the nadir view estimated for this sample at 395. Nevertheless, this calculus is only for this sample, the nadir position changes along the flight due to the aeroplane shift. Thus, the hot spot peak is reached at 15.7°-view zenith angle, which coincides with the SZA in an interval of about 2°, which is an acceptable difference due to errors in both the solar and the view zenith angles calculation.

Figure 12 shows the linear trend of the reflectance's gradient with the view zenith angle, which finishes very close to the backscattering where reflectance increases quickly and the hot spot peak appears. In this region the effects of the micro-scale and transmission through the cover became more important and govern the behaviour of the reflectance, [9]. The width and the amplitude of the hot spot signature, key to retrieving biophysical parameters, have been estimated trough the interception between the linear trend of the BRF and the vertical line crossing the hot spot peak.

In order to analyse the capability to obtain structural information from the hot spot directional signature acquired with HyMap we have calculated the angular width as it is shown in figure 12. For the alfalfa, V16, canopy the angular width γ is 1.4° and it is equal to LD/7H, in this case L is 3-4, H is 0.5-0.6 m and consequently, D can be calculated and is equal to 2-3 cm, which is an expected result for a alfalfa leaves. This result shows the capabilities of the HyMap instrument to derive information at leaf scales. On the other hand, we have checked the fact that the hot spot width is wavelength independent, which is in good agreement with results obtained from POLDER. However, results from space appear to point out that the hot spot width has not been so informative [9]. HyMap and POLDER airborne data can be very useful (joint extensive field campaigns) to determine with real data the information involved in the hot spot signature and their utility.

c) Solar Zenith Angle

In this section we have analysed how illumination geometry affects reflectance. We assumed again the azimuth isotropic behaviour in the illumination geometry. In order to reduce the viewing geometry influence on the reflectance, we have selected the images from the orthogonal plane. This configuration reduce the view zenith angle influence in the soils and very homogeneous cover, however for spare vegetation cover the gap effect determines that the view zenith angle can modify the radiometric response

We have selected several canopies with cover. The analyses of the sun zenith influence has been made from Bar2_9 and Bar1_12, thereby soil moisture could be artificially altered by irrigation system although in the fields studied this was not detected.

The wavelength dependence of the anisotropy introduced by the sun zenith angle is shown in figure 13 by means of the ANIF*i*.

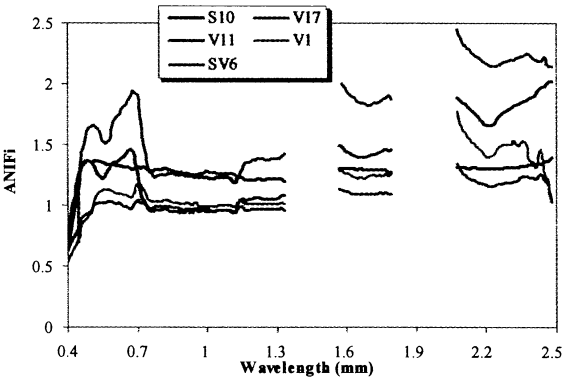

Fig.13. Anisotropy factor due to illumination angle between the noon and morning flights in the orthogonal plane.

Figure 13 shows very interesting aspects of the illumination influence in the BRF. For the smooth soil, S10, we can check that the ANIF*i* shows very close values to the field data analyses.

For the densest alfalfa cover, V17, the ANIF*i* is close to unity and preserves the wavelength dependence shown with the ANIF. This is again proof of the more isotropic behavior of the reflectance in vegetation that in soils. The other vegetation canopy analyzed with field data, the wheat V1, shows a slightly greater ANIF*i* value. Where the influence of the sun zenith angle is more evident is for the spare vegetation cover V11 (LAI=0.6) and SV6 LAI=0.8). Therefore, the soil contribution to the reflectance increases and so, the irradiation condition has a major influence. For a near horizon sun position as in the morning, shadows are bigger and vegetation is better illuminated, thus soil contribution decrease. The opposite case occurs when the sun is near nadir, therefore the shadows are lower and a higher fraction of soil contributes to the reflectance. Consequently, the ANIF*i* must be important where the soil and vegetation has a higher spectral contrast. Effectively, in the red regions and beyond 2000 nm is where the anisotropic behavior due to sun zenith angle has the highest values. This contrast between the anisotropy reflectance due to sun zenith angle in Red and NIR region can be useful to normalize soil contribution in arid or semiarid regions. This contrast appears for very low LAI levels, as in the SV6 and V11 where the LAI is lower than 1.0 and confirms the hypothesis that the angular information introduce new elements to normalize soil contribution, mainly, in arid or semi-arid environments [8].

Difference with the ANIF appears where water absorption is more important, around 1600 nm and beyond 2000 nm. These differences should be associated with the change in the moisture degree of the samples, although further research is needed to test the moisture effect on anisotropy reflectance.

CONCLUSIONS

During the Daisex-99 campaigns a set of flights were conducted with the HyMap instrument on board Do228

© European Space Agency • Provided by the NASA Astrophysics Data System

2001ESASP.499..163C

airborne. At the same time, the field radiometry team of the University of Valencia was acquired in situ data from nadir view at different time and off-nadir view in both the principal and the orthogonal plane. BRDF sampling was obtained with the FIGOS by the University of Zurich team. In this work, the anisotropic behavior of the BRF in both aforementioned viewing plane has been analyzed, comparing the field data with the HyMap airborne data.

Field measurements have demonstrated the strong difference between the orthogonal and the principal plane:

- In the orthogonal plane, for soils and very homogenous canopies there is little influence of the view zenith angle, and the BRF showing an isotropic behavior. This configuration is, in consequence, the most suitable for validation purpose of wide FOV sensors, and to interpret vegetation products derived from images not corrected of BRDF effects.
- In the principal plane, the broad hot spot signature has shown differences for the two homogeneous canopies, which is in agreement with the physical mechanism reported here.
- The wavelength dependence of the anisotropy factor reveals the strong structural difference between alfalfa and wheat crops, mainly where water absorption increase. The phenology status of wheat, completely spiked, has been identified as responsible for the atypical dense vegetation ANIF.

Airborne data analysis confirms the results from field data:

- We have checked the fact that in the orthogonal plane, for soils and homogeneous and dense canopies, reflectance can be considered isotropic with respect to view angle variations.
- In the principal plane, when the SZA is lower than the half-FOV of HyMap the hot spot has been obtained. Hence HyMap instrument allows us to acquire with high angular resolution the hot spot effect, which can be an important key to retrieve vegetation biophysical parameters such as LAI or canopy height.
- The sharper hot spot signature has been analysed, demonstrating the HyMap capabilities to determine the hot spot amplitude and width. Results have been in agreement with previous works, showing the wavelength independence of the width, which has been of 1.4°. Nevertheless, further research is needed to find relationships between the hot spot width and amplitude with the vegetation parameter. Flights with the HyMap joint to collection of field data, in a similar way to that of DAISEX campaigns, would be convenient.

- Finally, the wavelength dependence of the anisotropy due to sun zenith angle influence has been studied. Results seem to be in agreement with the reciprocity principle. The wavelength dependence of ANIF*i* shows significant difference where the spectral contrast between them is important. Furthermore, the ANIF*i* diverges more from ANIF where the water content in plant is more important, and could be an indicator of water stress for complete canopies.

REFERENCES

[1] Nicodemus, F.E., J.C. Richmond, J.J., Hsia, I.W. Ginsberg, F. Limperis, (1977). "Geometrical Considerations and Nomenclature for Reflectance". *National Bureau of Standards. NBS.* Monograph 160.

[2] Bicheron, P and M. Leroy, (2001). "BRDF of Major Biomes Observed from Space", *Journal Of Geophysical Research* (in press).

[3] Van Leeuwen, J.D and J.L. Roujean, (2001). "Improvement in BRDF Sampling and Albedo due to the Synergistic use of Geostationary and Polar Orbiting Satellite data", *Proceedings of the 8th Int. Symp. Physical Measurements & Signatures in Remote Sensing. Aussois. France. 8-12 January 2001.*

[4] Kimes, D.S., (1983). Dynamics of Directional Reflectance Factor Distributions for Vegetation Canopies. *Applied Optics*, vol. 22, n°.9:1364-1372.

[5] Camacho-de Coca, F., B. Martinez, M. A. Gilabert and J. Meliá (2001). Reflectance Anisotropy Analysis of Homogeneous Canopies Using Laboratory and Hymap Airborne Data. *Remote Sensing for Agriculture, Ecosystems, and Hydrology II. Barcelona 2000. SPIE.* Vol.4171: 280-291.

[6] Sandmeier et al., (1998). C. Müller, B. Hosgood and G. Andreoli, (1998-B) Physical mechanisms in Hyperspectral BRDF Data of Grass and Watercress. *Remote Sensing of Environment,* 66: 222-223.

[10] Qin, W. and Y. Xiang, (1994). On the Hotspot Effect of the Leaf Canopies: Modeling Study and Influence of Leaf Shape. *Remote Sensing of Environment,* 50: 95-106.

[11] Jupp, D.L.B. & A.H. Strahler (1991). A Hotspot Model for Leaf Canopies. *Remote Sensing of Environment,* 38:193-210.

[9] Breon, F.M., F. Maignan, M. Leroy and I. Grant (2001). A Statistical Analysis of Hot Spot directional signatures measured from space. *Proceedings of the 8th International Symposium: Physical Measurements and Signatures in Remote Sensing.* Aussois.

[8] Camacho-de Coca, F., M. A. Gilabert and J. Meliá (2001). Hot Spot Signature Dynamics with variyng LAI. *Proceedings of the 8th International Symposium: Physical Measurements and Signatures in Remote Sensing.* Aussois.

[7] Leblanc, S.G., J.M. Chen, P. White, J. Cihlar, R. Lacaze, J.L. Roujean and R. Latifovic (2001). Mapping Vegetation Clumping Index from Directional Satellites Measurements. *Proceedings of the 8th International Symposium: Physical Measurements and Signatures in Remote Sensing.* Aussois.

[12] Iqball, M.(1983). An introduction to Solar Radiation. *Academic Press*

© European Space Agency • Provided by the NASA Astrophysics Data System

2001ESASP.499..163C

© European Space Agency • Provided by the NASA Astrophysics Data System

The arm allows to turn 360° in the azimuth and to situate the sensor in the chosen view plane

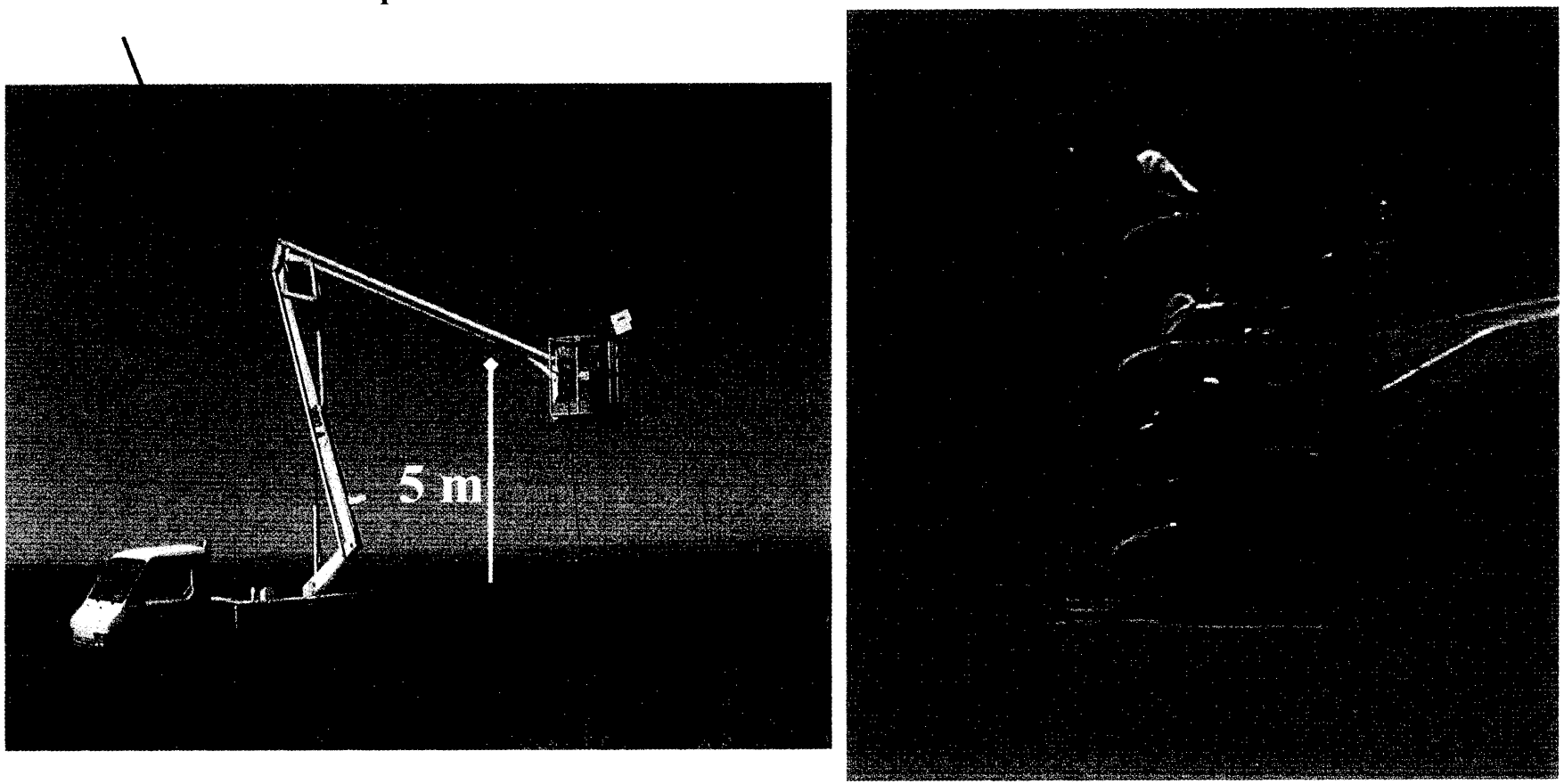

Plate1. Experimental methodology of angular measurements acquisition

2001ESASP.499..163C

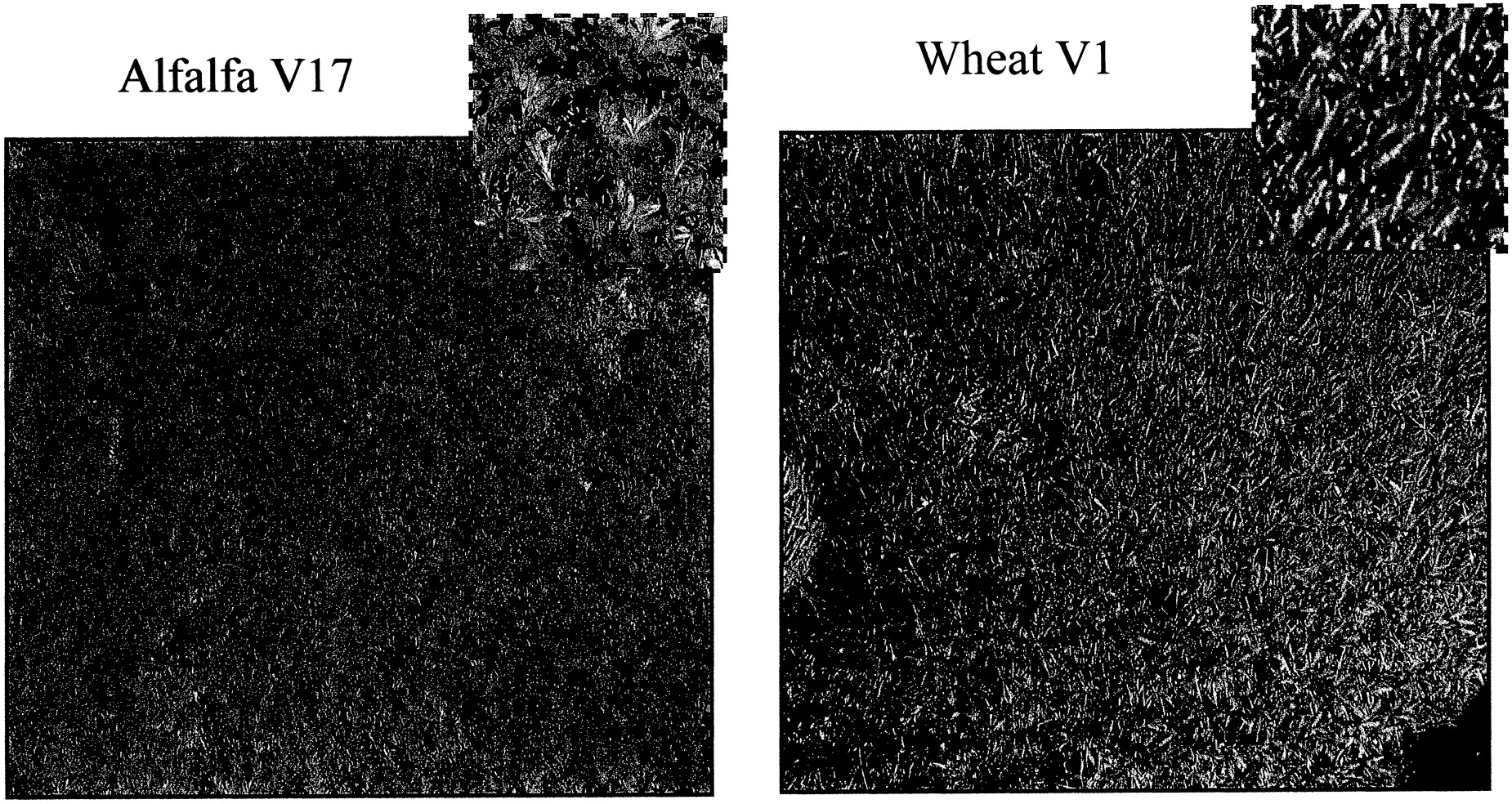

Plate2. Vegetation canopies selected for the angular measurements seen at 5-m height

© European Space Agency • Provided by the NASA Astrophysics Data System